


Original Research

HP1 Promotes the Centromeric Localization of ATRX and Protects Cohesion by Interfering Wapl Activity in Mitosis

Erchen Zhang^{1,2,†}, Lei Peng^{1,†}, Kejia Yuan¹, Zexian Ding¹, Qi Yi^{1,*} 

¹The Key Laboratory of Model Animals and Stem Cell Biology in Hunan Province, Hunan Normal University Health Science Center, 410013 Changsha, Hunan, China

²Central South University Institute of Reproduction and Stem Cell Engineering, 410013 Changsha, Hunan, China

*Correspondence: yiqi@hunnu.edu.cn (Qi Yi)

[†]These authors contributed equally.

Academic Editor: Alike K. Maunakea

Submitted: 4 September 2024 Revised: 2 November 2024 Accepted: 7 November 2024 Published: 21 January 2025

Abstract

Background: α thalassemia/mental retardation syndrome X-linked (ATRX) serves as a part of the sucrose nonfermenting 2 (SNF2) chromatin-remodeling complex. In interphase, ATRX localizes to pericentromeric heterochromatin, contributing to DNA double-strand break repair, DNA replication, and telomere maintenance. During mitosis, most ATRX proteins are removed from chromosomal arms, leaving a pool near the centromere region in mammalian cells, which is critical for accurate chromosome congression and sister chromatid cohesion protection. However, the function and localization mechanisms of ATRX at mitotic centromeres remain largely unresolved. **Methods:** The clustered regularly interspaced short palindromic repeats with CRISPR-associated protein 9 (CRISPR-Cas9) system and overexpression approaches were employed alongside immunofluorescence to investigate the mechanism of ATRX localization at the centromere. To study the binding mechanism between ATRX and heterochromatin protein 1 (HP1), both full-length and truncated mutants of hemagglutinin (HA)-ATRX were generated for co-immunoprecipitation and glutathione S-transferase (GST)-pull assays. Wild-type ATRX and HP1 binding-deficient mutants were created to investigate the role of ATRX binding to HP1 during mitosis, with the Z-Leu-Leu-Leu-al (MG132) maintenance assay, cohesion function assay, and kinetochore distance measurement. **Results and Conclusions:** Our research demonstrated that HP1 α , HP1 β , and HP1 γ facilitate the positioning of ATRX within the mitotic centromere area through their interaction with the first two [P/L]-X-V-X-[M/L/V] (PxVxL) motifs at the N-terminus of ATRX. ATRX deficiency causes aberrant mitosis and decreased centromeric cohesion. Furthermore, reducing Wapl activity can bypass the need for ATRX to protect centromeric cohesion. These results provide insights into the mechanism of ATRX's centromeric localization and its critical function in preserving centromeric cohesion by reducing Wapl activity in human cells.

Keywords: ATRX; HP1; cohesion; Wapl; chromosomal instability

1. Introduction

Chromosomal instability (CIN), serves as a defining characteristic of various cancers, arising from increased mis-segregation of chromosomes throughout mitosis [1,2]. CIN also drives tumor progression, metastasis [3], immune evasion [4,5], and multidrug resistance [6]. The precise segregation of chromosomes relies on a complex cellular network, with a crucial point being the cohesion of sister chromatids facilitated by the multisubunit cohesin complex. Cohesion defects are intricately linked to CIN [7,8]. Somatic cells possess two variants of the cohesin complex, composed of structural maintenance of chromosomes 1 (Smc1), structural maintenance of chromosomes 3 (Smc3), Rad21, and stromal antigen1/2 (SA1/ SA2) protein. During the cell cycle, two HEAT repeat-containing proteins, Pds5 cohesin-associated factor (Pds5) and Wapl, dynamically interact with cohesin to regulate its association with chromatin [9,10]. In the S phase, sister-chromatid cohesion is formed. Wapl, the antagonist of cohesin, dissociates most of the protein on the chromosomal arms when ver-

tebrate cells enter mitosis. However, to guarantee correct bi-orientation of chromosomes until the onset of anaphase, cohesin at centromeres including Sororin [11], shugoshin-like protein 1 (Sgo1) [12–17], heterochromatin protein 1 (HP1) [18], and Haspin [19,20] is protected from premature removal. The mechanisms responsible for the complete protection of centromeric cohesion from Wapl-dependent cohesin release during mitosis remain incompletely understood.

HP1, a crucial element of heterochromatin, is vital for gene silencing, transcriptional activation, DNA repair, chromosome segregation, and sister chromatid cohesion protection [18,21–23]. There are three unique isoforms of HP1 in mammalian cells, HP1 α , HP1 β , and HP1 γ , these isoforms exhibit a significant level of structural and functional similarity [24]. HP1 homologs possess two conserved regions: the N-terminal chromo domain (CD) and the C-terminal chromoshadow domain (CSD), which are joined by the Hinge domain [25–27]. The CD detects di- or trimethylation of lysine 9 in histone H3 (H3K9me2/3),



functioning as a transcriptional repressor and promotes the heterochromatin localization of HP1 [28]. Meanwhile, the CSD facilitates the dimerization of HP1, creating a hydrophobic interface that binds proteins possessing the [P/L]-X-V-X-[M/L/V] (PxVxL) motif, where X can be any amino acid [27]. Previous research suggests that HP1 α and HP1 γ share similar roles in maintaining centromeric cohesion by facilitating the localization of Haspin at mitotic centromeres in mammalian cells. Meanwhile, the necessity for HP1 in protecting sister chromatid cohesion can be circumvented by either directing Haspin to specific sites or by inhibiting the activity of Wapl [18].

α thalassemia/mental retardation syndrome X-linked (ATRX), a chromatin remodeling protein, belongs to the sucrose nonfermenting 2 (SNF2) helicase/ATPases family, which is believed to modulate gene expression by affecting chromatin structure and functionality. This protein was first discovered via a genetic defect causing X-linked syndrome disorder, which is characterized by severe psychomotor delays, genital abnormalities, unique facial characteristics, and α -thalassemia [29]. Mutations in the *ATRX* gene are widely distributed in gliomas, pancreatic neuroendocrine tumors (PanNETs), and acute myelocytic leukemia (AML) [30,31]. Depletion of ATRX in mammalian oocytes leads to abnormal chromosome morphology during meiosis, increased aneuploidy, and decreased fertility, indicating that ATRX is important in the formation of heterochromatin during mammalian meiosis [32]. ATRX is also critical for accurate chromosome congression and sister chromatid cohesion maintaining [33]. By binding to histone H3 trimethylated on lysine 9 (H3K9me3) and HP1, ATRX localizes to pericentromeric heterochromatin during interphase [34–36]. As cells proceed into mitosis, most of ATRX proteins released from the arms of chromosomes, with a little part remaining at the centromere region, which is similar to cohesion and HP1 [18,37,38]. However, the mechanisms governing the localization and functions of ATRX during mitosis remain largely unexplored.

2. Materials and Methods

2.1 Cell Culture

HeLa cells obtained from ATCC were cultured in Dulbecco's Modified Eagle Medium (DMEM) from Invitrogen (11965092, Carlsbad, CA, USA), enriched with 1% penicillin/streptomycin and 10% fetal bovine serum (FBS) sourced from Gibco (10091148, Auckland, New Zealand), and were kept at maintained at 37 °C with 5% CO₂. HeLa cells stably expressing hemagglutinin (HA)-ATRX (wild type (WT) or mutants) were selected and kept with 1.0 μ g/mL or 0.5 μ g/mL puromycin (NSC-3055, TargetMol, Shanghai, China). Clones 2A4 and 3A2 of HP1 DKO cells were previously described [18]. All cell lines were authenticated before use via short tandem repeat (STR) profiling to ensure their authenticity and reliability. Additionally, all

cell lines were confirmed to be mycoplasma-free using the GMyc-PCR Mycoplasma Detection Kit (40601, YEASEN, Shanghai, China).

2.2 Plasmids, siRNA, Transfection, and Drug Treatments

GST (glutathione S-transferase)-HP1 α , GST-HP1 α -I165E, GST-HP1 α -W174A, HP1 α -Flag-6xHis, HP1 β -Flag-6xHis, HP1 γ -Flag-6xHis, and pBos-centromere protein B (CB)-HP1 α -GFP were previously described [18]. HA-ATRX was kindly provided by professor Fangwei Wang (Zhejiang University). GST-HP1 β , GST-HP1 γ , GST-ATRX-L1 (561-610aa), GST-ATRX-L2 (1951-2000aa), GST-ATRX-L3 (171-220aa), GST-ATRX-L4 (1601-1650aa) were generated by inserting polymerase chain reaction (PCR) fragments into the pGEX-4T1-GST vector. HA-ATRX- Δ P1 and HA-ATRX- Δ PxVxL were created using Mut Express MultiS Fast Mutagenesis Kit (C215-01, Vazyme, Nanjing, China). Every plasmid was sequenced to ensure that no unwanted changes existed and that only desired mutations were found.

siATRX duplexes and control small interfering RNA (siRNA) (RiboBio, Guangzhou, China): *siATRX#1* (5'-GAGGAAACCUUCAUUGUAUU-3'), *siATRX#2* (5'-GUGGGCUGAAGAAUUUAAUdTdT-3'), *siWapl* (5'-CGGACUACCCUUAGCACAAdTdT-3'). Plasmid transfections employed Polyethyleneimine (19850, Polysciences, Warrington, PA, USA) or Eugene 6 (E2691, Promega, Madison, WI, USA), siRNA transfections employed Oligofectamine (12252011, Invitrogen, USA) and Lipofectamine RNAi MAX (13778150, Invitrogen, Carlsbad, CA, USA). 1.0 μ M nocodazole (R17934, MCE, Monmouth Junction, NJ, USA), 10 μ M MG132 (HY-13259, MCE, Monmouth Junction, NJ, USA) are used in this study. Selective detachment with “shake-off” facilitated the collection of mitotic cells.

2.3 Antibodies

Primary antibodies: rabbit polyclonal antibodies against ATRX (HPA001906, Sigma, St. Louis, MO, USA), Wapl (A300-268A, Bethyl, Montgomery, TX, USA), GFP (A11122, Invitrogen, USA), ACTB (PAB13193, abnova, Taiwan, China). Mouse monoclonal antibodies against HP1 α (MAB3584 for immunostaining; MAB3446 for immunoblotting, Millipore, Bedford, MA, USA), HP1 β (MAB3448, Millipore, USA), HP1 γ (MAB3450, Millipore, USA), HA (16B12, Biolegend, Beijing, China), Flag-tag (M2, Sigma, USA), GAPDH (YM3029, Immunoway, Plano, TX, USA). Guinea pigs polyclonal antibodies against centromere protein C (CENP-C) (PD030, MBL, Beijing, China).

Secondary antibodies: goat anti-rabbit IgG-HRP or horse anti-mouse (7074P2 or 7076P2, CST, Boston, MA, USA). Anti-mouse IgG-Alexa Fluor 488 or 555 (A-21202 or A-31570, Invitrogen, USA), anti-rabbit IgG-Alexa Fluor 488 or 555 (A-21206 or A-31572, Invitrogen, USA), anti-

guinea pig IgG-Alexa Fluor 555 (A-21435, Invitrogen, USA), all for immunostaining.

2.4 HP1 Gene Knockout in HeLa Cells

Single-guide RNA (sgRNA) was procured from Qingke (Beijing, China), then annealed and inserted into pX330 or pX462 plasmid from Addgene (110403 or 48141, Boston, MA, USA). After plasmids transfected HeLa cells for 48 hours, cells were individually split to establish clonal cell lines, puromycin was used to the selection process. HP1 triple knockout (TKO) clone H32-21 was obtained with sgRNA sequences, 5'-ACGTGTAGTGAATGGGAAAGtg-3' target to HP1 γ , 5'-CTTTGCCCTTTACCACTCGAcgg-3' and 5'-GGAGTACCTCCTAAAGTGGAagg-3' target to HP1 β , 5'-AGAACTGTCAGCTGTCCGCTtg-3' and 5'-GGAGGAGTATGTTGTGGAGAagg-3' target to HP1 α . For H23-19 clone, 5'-CTTTGCCCTTTACCACTCGAcgg-3' and 5'-GGAGTACCTCCTAAAGTGGAagg-3' target to HP1 β , 5'-TTTCCACGACAAATTCTTCagg-3' and 5'-CTAGATCGACGTGTAGTGAAtgg-3' target to HP1 γ , 5'-AGAACTGTCAGCTGTCCGCTtg-3' and 5'-GGAGGAGTATGTTGTGGAGAagg-3' target to HP1 α . HP1 knock out clones were identified by immunostaining and immunoblotting. pBluescript II KS (-) was used to subclone genomic DNA PCR fragments, which were then transformed into *E. coli*. To confirm the gene disruption, a select number of bacterial colonies were subsequently sequenced.

2.5 Fluorescence Microscopy, and Statistical Analysis

Cells were first fixed in 2% Paraformaldehyde (PFA, E672002, Sangon, Shanghai, China) in PBS for a duration of 20 minutes, then treated with 0.5% Triton X-100 (A110694, Sangon, Shanghai, China) in PBS for 5 minutes. For shake-off procedure, HeLa cells were re-attached to glass coverslips at 1500 rpm for 5 minutes by Cytospin. For chromosome spreads, mitotic cells were incubated in 75 mM KCl (A610440, Sangon, Shanghai, China) for 10 minutes, then reattaching them to glass coverslips using Cytospin, then fixed them like before. After fixation, cells were treated with 3% BSA (V900933, Sigma, USA) in PBS at room temperature for two hours with primary antibodies and one hour with secondary antibodies. Using DAPI (C1005, Beyotime, Shanghai, China), DNA staining was done for 5 minutes.

A fluorescent microscope (DM3000, Leica, Shanghai, China) was used to capture pictures. The centromere marker CENP-C was used to measure the inter-kinetochore (KT) distance, where over 20 kinetochores per cell were analyzed across a minimum of 15 cells. The distance was computed using the Leica LAS Live Measurement imaging software (Leica, Wetzlar, Germany). Images acquired under consistent illumination conditions, and fluorescent intensity was quantified of using ImageJ (NIH,

Bethesda, Maryland, USA). Specifically, within chromosome spreads, the average pixel intensity for ATRX and HP1 α staining at the inner centromeres, identified as areas within a circle of 3 pixels in diameter surrounding paired centromeres, was evaluated. The intensity of CENP-C was determined within a 9-pixel diameter circle that included individual centromere spots. The ratio of ATRX/anti-centromere antibody (ACA), ATRX/CENP-C, HP1 α /CENP-C, and HA-ATRX/CENP-C intensity was calculated for each centromere after background correction. Cohesion loss was defined as the separation of over 20% of sister-chromatid pairs within a single cell. Image editing was performed using Adobe Photoshop (Adobe, San Jose, CA, USA) and Illustrator (Adobe, USA). GraphPad Prism 10 (GraphPad Software, San Diego, CA, USA) was employed to do statistical analysis using unpaired *t*-tests.

2.6 Immunoblotting and Immunoprecipitation

Cell lysates were generated using either standard SDS sample buffer (B548118, Sangon, Shanghai, China) or P150 buffer intended for immunoblotting procedures. For co-immunoprecipitation purposes, cells underwent lysis in P150 buffer supplemented with 25 mM Tris-HCl (pH 7.5) (B548124, Sangon, Shanghai, China), 2 mM MgCl₂ (B601194, Sangon, Shanghai, China), 150 mM NaCl (A610476, Sangon, Shanghai, China), 1 mM dithiothreitol (DTT) (A620058, sangon, Shanghai, China), cocktail (P1005, Beyotime, Shanghai, China), 10 mM NaF (A500850, Sangon, Shanghai, China), 1 mM phenylmethanesulfonyl fluoride (PMSF) (ST505, Beyotime, Shanghai, China), 0.1 μ M okadaic acid (S1786, Beyotime, Shanghai, China) and 20 mM β -glycerophosphate (ST637, Beyotime, Shanghai, China). After high-speed centrifugation, GammaBind G Sepharose (28411301, GE Healthcare, Chicago, IL, USA) was used for lysates pre-clear. The lysates were then mixed with antibodies for 3 hours at 4 °C, followed by the addition of GammaBind G Sepharose for an additional hour. After being washed three times with the P150 lysis buffer, the beads were boiled with standard SDS sample buffer prior to immunoblotting analysis.

2.7 GST Pulldown

Plasmids that encode proteins fused to GST were introduced into BL21 cells (TSV-A09, Qingke, Beijing, China). These cells were cultivated until the optical density at 600 nm reached between 0.6 and 0.7. Protein expression was then initiated by adding 0.1 to 0.4 mM isopropyl β -D-thiogalactoside (IPTG, A100487, Sangon, Shanghai, China) and incubating at 16 °C for 16 hours. Following this, the cells were disrupted using sonication in a buffer solution containing 20 mM Tris-HCl (pH 8.0), 1 mM EDTA (B540625, Sangon, Shanghai, China), 100 mM NaCl, and 1% Triton X-100. The lysate was clarified through centrifugation and subsequently mixed with Glutathione Sepharose

4B (17075601, NEB, cytiva, Washington DC, USA) in the lysis buffer. The resin was then washed with lysis buffer.

For the pulldown of ATRX from lysates using GST-HP1 α (WT or mutants), mitotic HeLa cells expressing exogenous ATRX and arrested with nocodazole were lysed in a P150 buffer. The lysates were precleared with glutathione Sepharose 4B beads, followed by incubation with GST fusion proteins attached to the beads for 2 hours at 4 °C. The beads underwent three washes with the same buffer before being analyzed by immunoblotting or Coomassie Brilliant Blue (CBB) staining.

3. Results

3.1 HP1 Promotes Centromeric Localization of ATRX

In mammals, HP1 comprises three HP1 isoforms, HP1 α , HP1 β , and HP1 γ . Upon mitotic entrance, most of HP1 proteins are shifted from chromosome arms, while a fraction remains localized at the heterochromatic centromere region [39,40]. Our prior investigations revealed that both HP1 α and HP1 γ localize at the inner centromere, where they serve redundant functions in safeguarding centromeric cohesion in human cells [18]. According to immunofluorescence microscopy, ATRX localizes to heterochromatin during interphase and subsequently relocates to centromeres in mitotic HeLa cells. Notably, ATRX colocalizes with HP1 α during both mitosis and interphase (Fig. 1A). Interestingly, in HP1 α and HP1 γ double knockout (HP1 DKO) cell lines, the presence of centromeric ATRX was diminished by 30%–40%, with residual localization observed at the centromere (Fig. 1B,C).

Using CRISPR-associated protein 9 (CRISPR/Cas9) system [41–43], we generated two stable HP1 triple-knockout (HP1 TKO) clones, denoted as H23-19 and H23-21, in which different single-guide RNAs (sgRNAs) were used to individually knock out HP1 α , HP1 β , and HP1 γ [44]. Immunoblotting analysis has confirmed the depletion of the HP1 protein (Fig. 1D). Immunofluorescence microscopy revealed a more pronounced decrease in mitotic centromeric ATRX in HP1 TKO cells than in HP1 DKO cells, resulting in severe elimination of centromeric localization (Fig. 1E,F). In contrast to HeLa cells, ATRX localization at heterochromatin almost completely disappeared throughout interphase in HP1 TKO cells (**Supplementary Fig. 1A**). Additionally, endogenous (Fig. 1G,H) and exogenous (**Supplementary Fig. 1B,C**) ATRX were recruited to the centromere by transient expression of CB-HP1 α -GFP but not CB-GFP. Furthermore, the knockout of HP1 α , HP1 β , or HP1 γ alone did not compromise the centromeric localization of ATRX (**Supplementary Fig. 1D,E**). Meanwhile, the total ATRX protein level remained unaltered in both the HP1 DKO and TKO cell lines (**Supplementary Fig. 1F**).

These findings indicate that the localization of ATRX at inner centromeres during mitosis and heterochromatin foci in interphase relies on the presence of HP1 α , HP1 β ,

and HP1 γ . Importantly, ATRX knockdown did not affect the localization of HP1 proteins at centromeres (**Supplementary Fig. 1G–I**).

3.2 The N-terminal End of ATRX Interacts with HP1 α , HP1 β , and HP1 γ

Given that ATRX is unable to localize to the centromere in HP1 TKO cells, an interaction between HP1 and ATRX may be implied. In mitotic HeLa cell lysates, we showed that GST-HP1 α can effectively pull down endogenous ATRX (Fig. 2A). Furthermore, in nocodazole-arrested mitotic 293T cell lysates, a reciprocal co-immunoprecipitation (co-IP) was observed between HP1 α -Flag-6xHis, which was expressed exogenously, and HA-ATRX (Fig. 2B).

We subsequently investigated the interaction of ATRX with various HP1 isoforms (HP1 α , HP1 β , and HP1 γ) in mammalian cells. In mitotic HeLa cell lysates, we showed that HP1 α , HP1 β , and HP1 γ were linked to both exogenous and endogenous ATRX through co-immunoprecipitation and GST-pulldown assays (Fig. 2C–E). Conversely, endogenous ATRX is hardly to be extracted from mitotic cell lysates by the GST-HP1 α mutants I165E or W174A (Fig. 2F).

The impairment of ATRX in the co-immunoprecipitation with the HP1 α -W174A mutant strongly suggests that ATRX may harbor a PxVxL motif that engages with the hydrophobic pocket of the CSD dimer. Earlier research indicated that HP1 α has interactions with the ATRX region encompassing 586-LYVKL-590aa (P1 short) [34,38], our investigations revealed that the deletion of residues P1 short did not abolish the interaction between ATRX and HP1 α (Fig. 2G–I). Subsequent analysis identified three additional conserved potential PxVxL motifs: P2 (1977-PSVSL-1981aa), P3 (192-LQVLI-196aa), and P4 (1623-LVVCP-1627aa) in ATRX (**Supplementary Fig. 2A**). To investigate these motifs, we generated GST-fused fragments encompassing 50 aa of ATRX, which included the conserved P1, P2, P3, P4 motif, individually. These fragments were named GST-L1, GST-L2, GST-L3, and GST-L4. Our results revealed that GST-L1 and GST-L3 effectively pulled down exogenous HP1 α -Flag in mitotic HeLa cell lysates, but not GST-L2 or GST-L4 (**Supplementary Fig. 2B–E**). We subsequently constructed HA-ATRX- Δ PxVxL, in which both P1 and P3 of ATRX were deleted. This mutant exhibited a deficiency in co-immunoprecipitating with HP1 α -Flag (Fig. 2H). Additionally, we confirmed that HA-ATRX, but not the HA-ATRX- Δ PxVxL mutant was pulled down by GST-fused HP1 α (Fig. 2I). In summary, our data revealed that HP1 α , HP1 β , and HP1 γ interact with the N-terminus of ATRX through the two PxVxL motifs (586-LYVKL-590aa and 192-LQVLI-196aa).

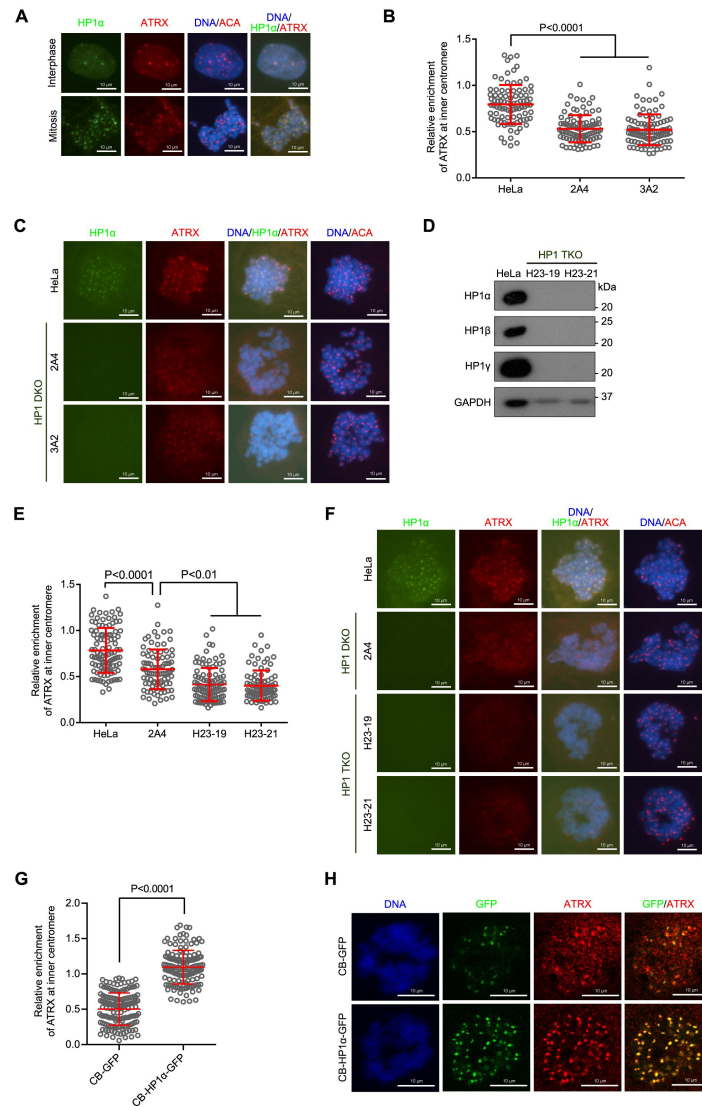


Fig. 1. HP1 promotes centromeric localization of ATRX. (A) Asynchronous HeLa cells were immunostained for interphase cells. Mitotic cells were collected by treated with nocodazole for 3 hours, then underwent cytopsin for immunostaining. (B,C) Cells were treated with nocodazole for a duration of 3 hours, after which the shake-off mitotic cells were subjected to immunostaining. The relative enrichment of ATRX was measured in across 10 cells (B) (analyzed using an unpaired *t*-test). Example images are shown in (C). (D) Immunoblot analysis was performed on asynchronous HeLa and the relevant HP1-TKO clones. (E,F) The stable cell lines specified underwent treatment with nocodazole for a duration of 3 hours, after which the shake-off mitotic cells were subjected to immunostaining. The relative enrichment of ATRX was measured in across 10 cells (E) (analyzed using an unpaired *t*-test). Representative images are supplied in (F). (G,H) HeLa cells were transiently transfected with either centromere protein B (CB)-GFP or CB-HP1 α -GFP, and the shake-off mitotic cells arrested with nocodazole were subjected to immunostaining. The ratio of centromeric ATRX/GFP immunofluorescence intensity was determined in across 10 different cells (G) (analyzed using an unpaired *t*-test), and example images are given (H). Data details: The means and standard deviations (SDs) are presented (B,E,G). Scale bars: 10 μ m. For further details, refer to **Supplementary Fig. 2**. ATRX, α thalassemia/mental retardation syndrome X-linked; HP1, heterochromatin protein 1; TKO, triple-knockout; ACA, anti-centromere antibody; GFP, green fluorescent protein.

3.3 Disruption of the HP1-ATRX Interaction Delocalizes ATRX from Mitotic Centromeres, Resulting in Increased Centromeric Cohesion Defects

ATRX directly interacts with HP1, and HP1 facilitates the centromeric localization of ATRX. The loss of ATRX is correlated with impaired centromeric cohesion and in-

creased chromosome segregation errors. This observation led us to explore the potential involvement of the HP1-ATRX interaction in both the centromeric localization of ATRX and its function in regulating sister chromatid cohesion.

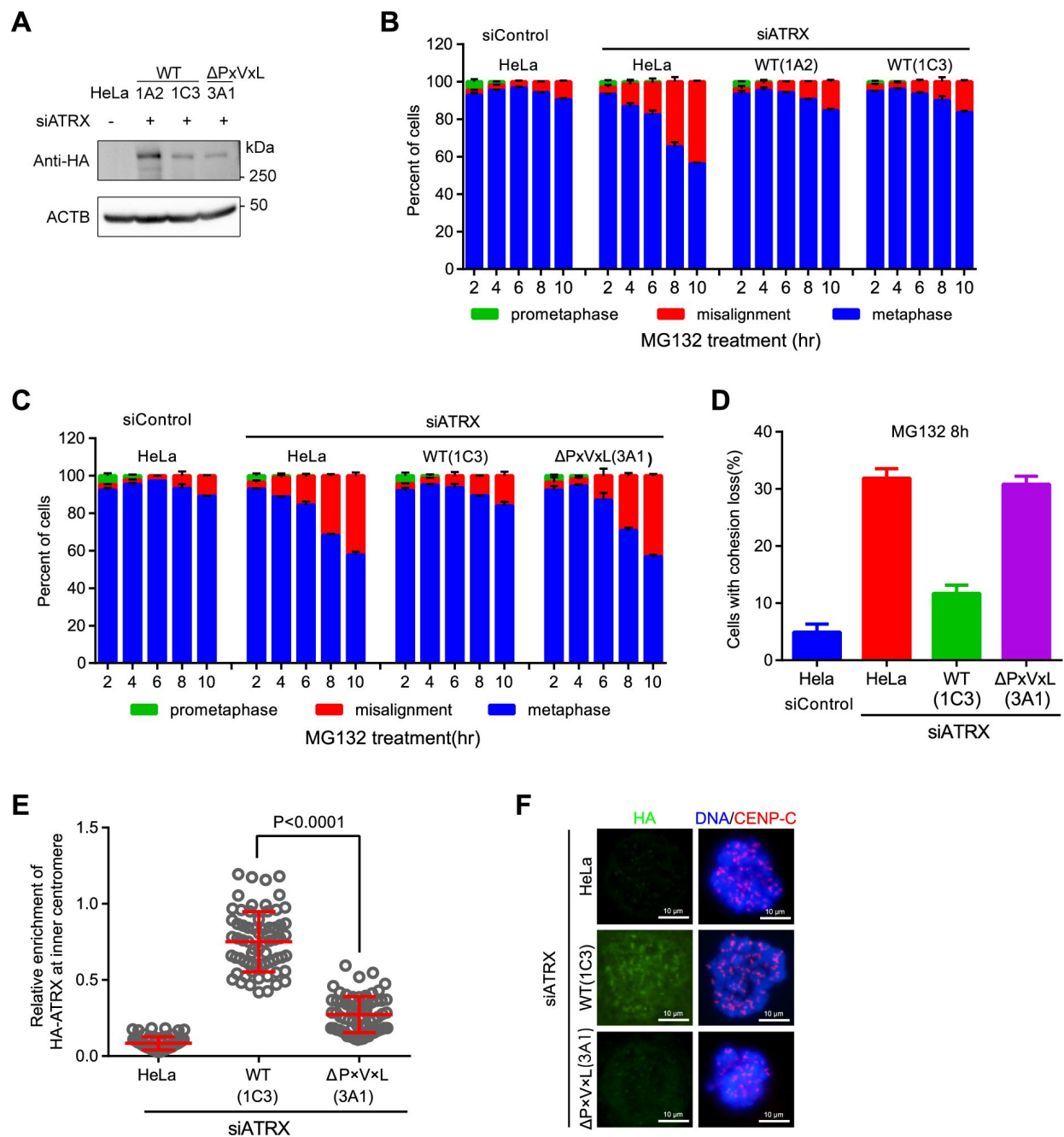


Fig. 3. Disruption of the HP1- ATRX interaction delocalizes ATRX from mitotic centromeres, resulting in increased centromeric cohesion defects. (A) Immunoblotting was performed on lysates derived from asynchronous HeLa cells along with the specified stable cell lines. (B,C) The specified stable cell lines as described in A underwent treatment with MG132, with or without the inclusion of endogenous ATRX RNAi cells. Cells were fixed at the given time intervals for DNA staining, and about 200 cells were counted ($n = 2$). (D) HeLa along with the referenced stable cell lines as described in A were treated with MG132 for 8 hours. The fraction of cells exhibiting cohesion loss was assessed in approximately 200 cells ($n = 2$) via mitotic chromosome spreads. Sample pictures are shown in **Supplementary Fig. 3C**. (E,F) The specified cell lines underwent a 3-hour treatment with nocodazole. The immunostaining of mitotic chromosome spreads was performed, and the ratio of immunofluorescence intensity for centromeric HA/CENP-C was measured in across 10 cells (E) (analyzed using an unpaired t -test). Example images are depicted in (F). Data information: Mean values and standard deviations (SDs) are displayed (B,C,E). Scale bar: 10 μ m. Refer to **Supplementary Fig. 3** for more information. WT, wild type; siControl, small interfering RNA Control.

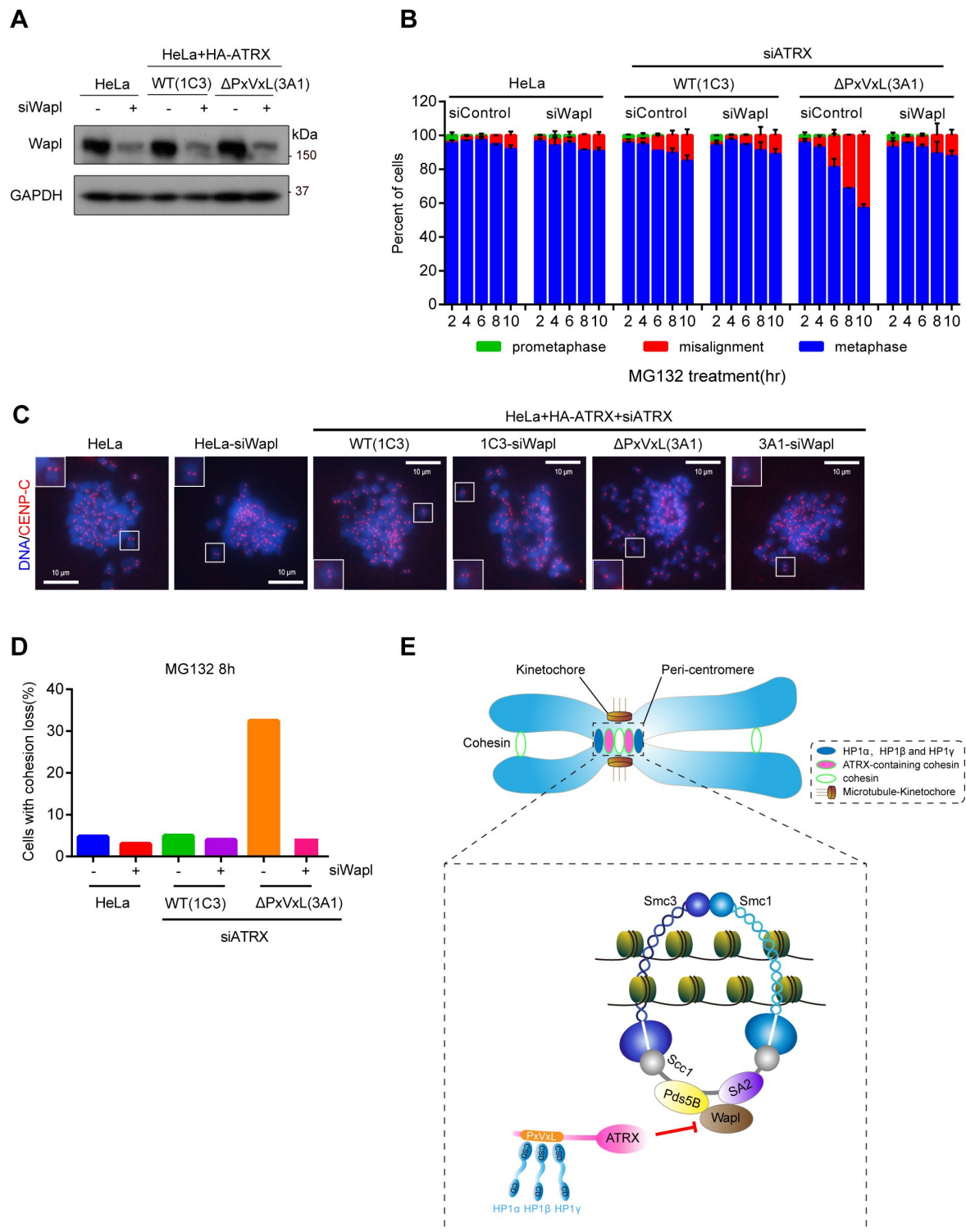


Fig. 4. Depletion of Wapl abolishes the need for the HP1-ATRX interaction in safeguarding centromeric cohesion. (A) Cell lines were transfected with the specified siRNAs and subjected to immunoblotting. (B) The selected cell lines expressing the indicated siRNAs were treated with MG132, fixed at predetermined time points, and analyzed in approximately 200 cells ($n = 2$). Means and standard deviations (SDs) were recorded. (C,D) HeLa cells and the specified cell lines received MG132 treatment for 8 hours. By utilizing mitotic chromosome spreads, the fraction of cells with cohesion loss was assessed in around 100 cells (C). Example images of the mitotic chromosome spreads are provided (D). Scale bar, 10 μ m. (E) Model for HP1 in localizing ATRX at mitotic centromeres, which inhibits Wapl's release of cohesin from mitotic centromeres.

To determine the functional importance of the HP1-ATR α interaction, we generated an ATR α siRNA-resistant plasmid and subsequently expressed wild-type HA-ATR α (1A2 and 1C3) and the HP1-binding-deficient mutant HA-ATR α - Δ PxVxL (3A1) in HeLa cells (Fig. 3A).

Endogenous ATR α protein was knocked down by siRNA duplexes. Following MG132-induced metaphase arrest, cells lacking ATR α presented pronounced deficiencies in maintaining correct chromosomal biorientation and sister chromatid cohesion. Importantly, these defects were efficiently rescued by the presence of HA-ATR α , but not by HA-ATR α - Δ PxVxL (Fig. 3B–D, **Supplementary Fig. 3A–C**).

Immunofluorescence microscopy additionally demonstrated that the exogenous expression of HA-ATR α , while not HA-ATR α - Δ PxVxL, promoted the centromeric localization of HA-ATR α when endogenous ATR α was absent (Fig. 3E,F). These findings emphasize the importance of the HP1-ATR α interaction in preserving centromeric cohesion during mitosis and in promoting the appropriate localization of ATR α .

3.4 Depletion of Wapl Abolishes the Need for the HP1-ATR α Interaction in Safeguarding Centromeric Cohesion

ATR α RNAi triggers a loss of cohesion, these findings underscore the significance of ATR α -interacting proteins in the protection of cohesion mediated by ATR α . Considering that the disruption of ATR α localization weakens sister chromatid cohesion, we hypothesized that the abnormal increase in local Wapl activity, resulting from the delocalization of centromeric ATR α , which we speculated would be a contributing factor to the centromeric cohesion abnormalities seen in ATR α -RNAi cells. siRNA duplexes were employed to knock down the endogenous ATR α protein, following MG132-induced metaphase arrest, our findings indicated that Wapl knockdown by siRNA significantly prevented the misalignment of metaphase chromosomes in cells expressing HA-ATR α - Δ PxVxL (Fig. 4A,B). Similarly, these mutant cells demonstrated the ability to sustain sister chromatid cohesion even without Wapl (Fig. 4C,D). Hence, the depletion of Wapl eliminates the need for HP1-ATR α interactions to maintain centromeric cohesion.

4. Discussion

The ATR α protein is pivotal for maintaining chromatin structure and regulating gene transcription [29]. Using immunofluorescence experiments, we confirmed the localization of ATR α in the heterochromatin region during interphase and its localization at the centromere during mitosis. ATR α -depleted cells generated by siRNA exhibited increased chromosome segregation errors and premature sister chromatid cohesion, consistent with previous findings [33]. These phenotypes are closely linked to increased chromosomal instability, which serves as both a cause and

a manifestation of tumorigenesis and metastasis. These observations displayed the vital role of ATR α in ensuring the faithful transmission of genetic information.

Shigeki Iwase *et al.* [34] demonstrated that the localization of ATR α at interphase heterochromatin relies on its recognition of H3K9me3 and its interaction with HP1 α in human cells. Moreover, during mitosis, ATR α interacts with HP1 α [38]. These findings were confirmed by our investigation, which also showed that HP1 α , HP1 β , and HP1 γ are essential for ATR α 's centromeric localization during mitosis and its positioning at heterochromatin foci during interphase. Previously, we reported that HP1 α and HP1 γ localized at the mitotic centromere, whereas HP1 β did not [18]. Knocking out HP1 β in HP1 double-knockout (HP1 α and HP1 γ) cell lines further reduced the localization of ATR α at the centromere. The underlying molecular mechanism underlying the absence of HP1 β at the mitotic centromere while influencing ATR α localization warrants further investigation.

It has long been known that HP1 α binds to the 586-LYVKL-590aa motif on ATR α [38]. However, we discovered that mutating the 586-LYVKL-590 motif of ATR α alone does not disrupt its binding to HP1. Instead, HP1 ensures the complete localization of ATR α at the mitotic site by binding to two PxVxL motifs, 192-LQVLI-196aa, and 586-LYVKL-590aa, at the N-terminal end of ATR α , thereby safeguarding centromere cohesion. Intriguingly, Wapl depletion rescues cohesion fatigue in the absence of ATR α -HP1 interaction. However, it is not clear which component of cohesion directly combines with ATR α and how to play a sister chromatid cohesion protection role.

5. Conclusions

Taken together, our findings indicate that HP1 ensures appropriate ATR α localization at the mitotic centromere, hence safeguarding centromeric cohesion and preventing chromosomal instability. Additionally, the ATR α -HP1 interaction suppresses Wapl activity. This antagonistic relationship inhibits the premature elimination of centromeric cohesion, ensuring sufficient cohesion maintenance at centromeres (Fig. 4E).

Availability of Data and Materials

The datasets used and/or analyzed during the current study are available from the corresponding author upon reasonable request.

Author Contributions

ECZ and LP designed and performed most of the experiments and analysis with the contributions from KJY, and ZXD. QY conceived and supervised the project designed the experiments, QY designed the experiments, analyzed the data, and wrote the manuscript. All authors contributed to editorial changes in the manuscript. All authors

read and approved the final manuscript. All authors have participated sufficiently in the work and agreed to be accountable for all aspects of the work.

Ethics Approval and Consent to Participate

Not applicable.

Acknowledgment

We thank Fangwei Wang (Zhejiang University) for kindly providing some of the plasmids and reagents. Thanks to Zuping He (Hunan Normal University) for providing us with an experimental platform.

Funding

This work was funded by grants from the National Natural Science Foundation of China (32000499) and the Natural Science Foundation of Hunan Provincial of China (2021JJ40346).

Conflict of Interest

The authors declare no conflict of interest.

Supplementary Material

Supplementary material associated with this article can be found, in the online version, at <https://doi.org/10.31083/FBL26426>.

References

- [1] Bakhoum SF, Cantley LC. The Multifaceted Role of Chromosomal Instability in Cancer and Its Microenvironment. *Cell*. 2018; 174: 1347–1360. <https://doi.org/10.1016/j.cell.2018.08.027>.
- [2] Drews RM, Hernando B, Tarabichi M, Haase K, Lesluyes T, Smith PS, *et al.* A pan-cancer compendium of chromosomal instability. *Nature*. 2022; 606: 976–983. <https://doi.org/10.1038/s41586-022-04789-9>.
- [3] Bakhoum SF, Ngo B, Laughney AM, Cavallo JA, Murphy CJ, Ly P, *et al.* Chromosomal instability drives metastasis through a cytosolic DNA response. *Nature*. 2018; 553: 467–472. <https://doi.org/10.1038/nature25432>.
- [4] Li J, Hubisz MJ, Earlie EM, Duran MA, Hong C, Varela AA, *et al.* Non-cell-autonomous cancer progression from chromosomal instability. *Nature*. 2023; 620: 1080–1088. <https://doi.org/10.1038/s41586-023-06464-z>.
- [5] Davoli T, Uno H, Wooten EC, Elledge SJ. Tumor aneuploidy correlates with markers of immune evasion and with reduced response to immunotherapy. *Science (New York, N.Y.)*. 2017; 355: eaaf8399. <https://doi.org/10.1126/science.aaf8399>.
- [6] Lee AJX, Endesfelder D, Rowan AJ, Walther A, Birkbak NJ, Futreal PA, *et al.* Chromosomal instability confers intrinsic multidrug resistance. *Cancer Research*. 2011; 71: 1858–1870. <https://doi.org/10.1158/0008-5472.CAN-10-3604>.
- [7] Barber TD, McManus K, Yuen KWY, Reis M, Parmigiani G, Shen D, *et al.* Chromatid cohesion defects may underlie chromosome instability in human colorectal cancers. *Proceedings of the National Academy of Sciences of the United States of America*. 2008; 105: 3443–3448. <https://doi.org/10.1073/pnas.0712384105>.
- [8] Elbatsh AMO, Medema RH, Rowland BD. Genomic stability: boosting cohesion corrects CIN. *Current Biology: CB*. 2014; 24: R571–R573. <https://doi.org/10.1016/j.cub.2014.05.009>.
- [9] Shintomi K, Hirano T. Releasing cohesin from chromosome arms in early mitosis: opposing actions of Wapl-Pds5 and Sgo1. *Genes & Development*. 2009; 23: 2224–2236. <https://doi.org/10.1101/gad.1844309>.
- [10] Carretero M, Ruiz-Torres M, Rodríguez-Corsino M, Barthelemy I, Losada A. Pds5B is required for cohesion establishment and Aurora B accumulation at centromeres. *The EMBO Journal*. 2013; 32: 2938–2949. <https://doi.org/10.1038/emboj.2013.230>.
- [11] Nishiyama T, Ladurner R, Schmitz J, Kreidl E, Schleiffer A, Bhaskara V, *et al.* Sororin mediates sister chromatid cohesion by antagonizing Wapl. *Cell*. 2010; 143: 737–749. <https://doi.org/10.1016/j.cell.2010.10.031>.
- [12] Ouyang Z, Zheng G, Tomchick DR, Luo X, Yu H. Structural Basis and IP6 Requirement for Pds5-Dependent Cohesin Dynamics. *Molecular Cell*. 2016; 62: 248–259. <https://doi.org/10.1016/j.molcel.2016.02.033>.
- [13] Liu H, Rankin S, Yu H. Phosphorylation-enabled binding of SGO1-PP2A to cohesin protects sororin and centromeric cohesion during mitosis. *Nature Cell Biology*. 2013; 15: 40–49. <https://doi.org/10.1038/ncb2637>.
- [14] Hara K, Zheng G, Qu Q, Liu H, Ouyang Z, Chen Z, *et al.* Structure of cohesin subcomplex pinpoints direct shugoshin-Wapl antagonism in centromeric cohesion. *Nature Structural & Molecular Biology*. 2014; 21: 864–870. <https://doi.org/10.1038/nsmb.2880>.
- [15] Rankin S, Ayad NG, Kirschner MW. Sororin, a substrate of the anaphase-promoting complex, is required for sister chromatid cohesion in vertebrates. *Molecular Cell*. 2005; 18: 185–200. <https://doi.org/10.1016/j.molcel.2005.03.017>.
- [16] Nishiyama T, Sykora MM, Huis in 't Veld PJ, Mechtler K, Peters JM. Aurora B and Cdk1 mediate Wapl activation and release of acetylated cohesin from chromosomes by phosphorylating Sororin. *Proceedings of the National Academy of Sciences of the United States of America*. 2013; 110: 13404–13409. <https://doi.org/10.1073/pnas.1305020110>.
- [17] Schmitz J, Watrin E, Lénárt P, Mechtler K, Peters JM. Sororin is required for stable binding of cohesin to chromatin and for sister chromatid cohesion in interphase. *Current Biology: CB*. 2007; 17: 630–636. <https://doi.org/10.1016/j.cub.2007.02.029>.
- [18] Yi Q, Chen Q, Liang C, Yan H, Zhang Z, Xiang X, *et al.* HP1 links centromeric heterochromatin to centromere cohesion in mammals. *EMBO Reports*. 2018; 19: e45484. <https://doi.org/10.15252/embr.201745484>.
- [19] Zhou L, Liang C, Chen Q, Zhang Z, Zhang B, Yan H, *et al.* The N-Terminal Non-Kinase-Domain-Mediated Binding of Haspin to Pds5B Protects Centromeric Cohesion in Mitosis. *Current Biology: CB*. 2017; 27: 992–1004. <https://doi.org/10.1016/j.cub.2017.02.019>.
- [20] Liang C, Chen Q, Yi Q, Zhang M, Yan H, Zhang B, *et al.* A kinase-dependent role for Haspin in antagonizing Wapl and protecting mitotic centromere cohesion. *EMBO Reports*. 2018; 19: 43–56. <https://doi.org/10.15252/embr.201744737>.
- [21] Saint-André V, Batsché E, Rachez C, Muchardt C. Histone H3 lysine 9 trimethylation and HP1 γ favor inclusion of alternative exons. *Nature Structural & Molecular Biology*. 2011; 18: 337–344. <https://doi.org/10.1038/nsmb.1995>.
- [22] Lucio RF, Allo M, Schor IE, Kornblitt AR, Misteli T. Epigenetics in alternative pre-mRNA splicing. *Cell*. 2011; 144: 16–26. <https://doi.org/10.1016/j.cell.2010.11.056>.
- [23] Ruppert JG, Samejima K, Platani M, Molina O, Kimura H, Jeyapakash AA, *et al.* HP1 α targets the chromosomal passenger complex for activation at heterochromatin before mitotic entry. *The EMBO Journal*. 2018; 37: e97677. <https://doi.org/10.15252/emboj.201797677>.
- [24] Ma J, Hwang KK, Worman HJ, Courvalin JC, Eissenberg JC. Expression and functional analysis of three isoforms of hu-

- man heterochromatin-associated protein HP1 in *Drosophila*. *Chromosoma*. 2001; 109: 536–544. <https://doi.org/10.1007/s004120000113>.
- [25] Paro R, Hogness DS. The Polycomb protein shares a homologous domain with a heterochromatin-associated protein of *Drosophila*. *Proceedings of the National Academy of Sciences of the United States of America*. 1991; 88: 263–267. <https://doi.org/10.1073/pnas.88.1.263>.
- [26] Aasland R, Stewart AF. The chromo shadow domain, a second chromo domain in heterochromatin-binding protein 1, HP1. *Nucleic Acids Research*. 1995; 23: 3168–3173. <https://doi.org/10.1093/nar/23.16.3168>.
- [27] Liu Y, Qin S, Lei M, Tempel W, Zhang Y, Loppnau P, *et al*. Peptide recognition by heterochromatin protein 1 (HP1) chromoshadow domains revisited: Plasticity in the pseudosymmetric histone binding site of human HP1. *The Journal of Biological Chemistry*. 2017; 292: 5655–5664. <https://doi.org/10.1074/jbc.M116.768374>.
- [28] Lachner M, O'Carroll D, Rea S, Mechtler K, Jenuwein T. Methylation of histone H3 lysine 9 creates a binding site for HP1 proteins. *Nature*. 2001; 410: 116–120. <https://doi.org/10.1038/35065132>.
- [29] Gibbons RJ, Picketts DJ, Villard L, Higgs DR. Mutations in a putative global transcriptional regulator cause X-linked mental retardation with alpha-thalassemia (ATR-X syndrome). *Cell*. 1995; 80: 837–845. [https://doi.org/10.1016/0092-8674\(95\)90287-2](https://doi.org/10.1016/0092-8674(95)90287-2).
- [30] Elsässer SJ, Allis CD, Lewis PW. Cancer. New epigenetic drivers of cancers. *Science (New York, N.Y.)*. 2011; 331: 1145–1146. <https://doi.org/10.1126/science.1203280>.
- [31] Jiao Y, Shi C, Edil BH, de Wilde RF, Klimstra DS, Maitra A, *et al*. DAXX/ATRAX, MEN1, and mTOR pathway genes are frequently altered in pancreatic neuroendocrine tumors. *Science (New York, N.Y.)*. 2011; 331: 1199–1203. <https://doi.org/10.1126/science.1200609>.
- [32] De La Fuente R, Baumann C, Viveiros MM. Chromatin structure and ATRX function in mouse oocytes. *Results and Problems in Cell Differentiation*. 2012; 55: 45–68. https://doi.org/10.1007/978-3-642-30406-4_3.
- [33] Ritchie K, Seah C, Moulin J, Isaac C, Dick F, Bérubé NG. Loss of ATRX leads to chromosome cohesion and congression defects. *The Journal of Cell Biology*. 2008; 180: 315–324. <https://doi.org/10.1083/jcb.200706083>.
- [34] Iwase S, Xiang B, Ghosh S, Ren T, Lewis PW, Cochrane JC, *et al*. ATRX ADD domain links an atypical histone methylation recognition mechanism to human mental-retardation syndrome. *Nature Structural & Molecular Biology*. 2011; 18: 769–776. <https://doi.org/10.1038/nsmb.2062>.
- [35] Eustermann S, Yang JC, Law MJ, Amos R, Chapman LM, Jelin-ska C, *et al*. Combinatorial readout of histone H3 modifications specifies localization of ATRX to heterochromatin. *Nature Structural & Molecular Biology*. 2011; 18: 777–782. <https://doi.org/10.1038/nsmb.2070>.
- [36] Bérubé NG, Smeenk CA, Picketts DJ. Cell cycle-dependent phosphorylation of the ATRX protein correlates with changes in nuclear matrix and chromatin association. *Human Molecular Genetics*. 2000; 9: 539–547. <https://doi.org/10.1093/hmg/9.4.539>.
- [37] Hayakawa T, Haraguchi T, Masumoto H, Hiraoka Y. Cell cycle behavior of human HP1 subtypes: distinct molecular domains of HP1 are required for their centromeric localization during interphase and metaphase. *Journal of Cell Science*. 2003; 116: 3327–3338. <https://doi.org/10.1242/jcs.00635>.
- [38] McDowell TL, Gibbons RJ, Sutherland H, O'Rourke DM, Bickmore WA, Pombo A, *et al*. Localization of a putative transcriptional regulator (ATRX) at pericentromeric heterochromatin and the short arms of acrocentric chromosomes. *Proceedings of the National Academy of Sciences of the United States of America*. 1999; 96: 13983–13988. <https://doi.org/10.1073/pnas.96.24.13983>.
- [39] Hirota T, Lipp JJ, Toh BH, Peters JM. Histone H3 serine 10 phosphorylation by Aurora B causes HP1 dissociation from heterochromatin. *Nature*. 2005; 438: 1176–1180. <https://doi.org/10.1038/nature04254>.
- [40] Fischle W, Tseng BS, Dormann HL, Ueberheide BM, Garcia BA, Shabanowitz J, *et al*. Regulation of HP1-chromatin binding by histone H3 methylation and phosphorylation. *Nature*. 2005; 438: 1116–1122. <https://doi.org/10.1038/nature04219>.
- [41] Cong L, Ran FA, Cox D, Lin S, Barretto R, Habib N, *et al*. Multiplex genome engineering using CRISPR/Cas systems. *Science (New York, N.Y.)*. 2013; 339: 819–823. <https://doi.org/10.1126/science.1231143>.
- [42] Ran FA, Hsu PD, Lin CY, Gootenberg JS, Konermann S, Trevino AE, *et al*. Double nicking by RNA-guided CRISPR Cas9 for enhanced genome editing specificity. *Cell*. 2013; 154: 1380–1389. <https://doi.org/10.1016/j.cell.2013.08.021>.
- [43] Mali P, Yang L, Esvelt KM, Aach J, Guell M, DiCarlo JE, *et al*. RNA-guided human genome engineering via Cas9. *Science (New York, N.Y.)*. 2013; 339: 823–826. <https://doi.org/10.1126/science.1232033>.
- [44] Wang T, Wei JJ, Sabatini DM, Lander ES. Genetic screens in human cells using the CRISPR-Cas9 system. *Science (New York, N.Y.)*. 2014; 343: 80–84. <https://doi.org/10.1126/science.1246981>.